Collapse of the random-phase approximation: Examples and counter-examples from the shell model

Calvin W. Johnson
Department of Physics, San Diego State University, 5500 Campanile Drive, San Diego, California 92182-1233, USA

Ionel Stetcu
Department of Physics, University of Washington, Box 351560, Seattle, Washington 98195-1560, USA

(Received 17 July 2009; published 31 August 2009)

The Hartree-Fock approximation to the many-fermion problem can break exact symmetries, and in some cases by changing a parameter in the interaction one can drive the Hartree-Fock minimum from a symmetry-breaking state to a symmetry-conserving state (also referred to as a "phase transition" in the literature). The order of the transition is important when one applies the random-phase approximation (RPA) to the of the Hartree-Fock wave function: if first order, RPA is stable through the transition, but if second-order, then the RPA amplitudes become large and lead to unphysical results. The latter is known as "collapse" of the RPA. While the difference between first- and second-order transitions in the RPA was first pointed out by Thouless, we present for the first time nontrivial examples of both first- and second-order transitions in a uniform model, the interacting shell-model, where we can compare to exact numerical results.

DOI: 10.1103/PhysRevC.80.024320 PACS number(s): 21.60.Cs, 21.60.Jz

I. INTRODUCTION

An important class of approximations in many-body theory are the mean-field approximations, which reduce the many-body problem to an effective one-body problem, and their generalizations [1]. In this article we consider the Hartree-Fock approximation, a variational approach that approximates the ground-state wave function by a single Slater determinant (antisymmeterized product of single-particle wave functions), and the random-phase approximation (RPA), which builds small amplitude correlations on top of the Hartree-Fock state and which itself can be derived as the small-amplitude limit of the *time-dependent* Hartree-Fock approximation.

Because the Hartree-Fock (HF) state ignores correlations, it can break exact symmetries, such as translational and rotational invariance. A related approximation, the Hartree-Fock-Bogoliubov (HFB) approximation, built on quasiparticles, also breaks conservation of the number of particles. Despite this breaking of symmetries, HF, HFB, and the RPA and quasiparticle RPA are widely and successfully used to describe low-energy nuclear structure.

If one dials the parameters of the Hamiltonian, it is possible for the ground-state HF or HFB wave function to change from a symmetry-preserving state to one that breaks an exact symmetry. For example, as one changes the single-particle energies as one attempts to fit data, the HF state may go between spherical and deformed states, and the HFB state may between normal (number-conserving) and superfluid (number-nonconserving) states.

A long time ago Thouless pointed out [2,3] that, as the mean-field state is driven between symmetry-conserving (SC) and symmetry-nonconserving (SNC) states, there are two possible kinds of state transitions (often referred to as "phase transitions" in the literature, even for finite systems). For second-order transitions the fluctuations in RPA become unphysically large, leading to the so-called collapse of the RPA. A frequently cited example is the collapse of RPA in the Lipkin-Meshkov-Glick model [4]. Significant effort in the literature has been devoted to collapse in the RPA and QRPA and possible solutions. All but forgotten are first-order transitions for which RPA does *not* collapse.

In this article we use a nontrivial realization of the HF and RPA in the interacting shell model, where we can compare to exact numerical calculations and demonstrate both first- and second-order transitions. As predicted by Thouless, second-order transitions and collapse are driven by odd-parity operators or modes, while first-order transitions are driven by even-parity operators or modes. In this article we do not propose any new solutions to the collapse of RPA at or near second-order transitions; instead, this work illustrates that the world of RPA and state transitions is more complicated than the standard narrative.

II. HARTREE-FOCK AND RPA CALCULATIONS IN THE INTERACTING SHELL MODEL

We work in the framework of the interacting shell model. The model space is defined by a truncated set of single-particle orbits, for example, the $0p_{1/2}$-$0p_{3/2}$ space, usually called the p shell, or the $1s_{1/2}$-$0d_{3/2}$-$0d_{5/2}$ space, the sd shell. The interaction is given by a set of single-particle energies ϵ_a and two-body matrix elements $V_{JT}(ab,cd)$. The interactions used are not necessarily simple schematic forces but generally start from carefully computed G-matrix interactions and then adjusted empirically to reproduce a large number of ground-state binding energies and excitation energies.

There are a number of computer programs that read in the model space, generate many-body basis states (Slater determinants in occupation space), compute the many-body matrix elements from the single-particle energies and two-body matrix elements, and diagonalize the Hamiltonian matrix to get out the eigenenergies and wave functions, from which one can compute observables, transitions, and so on. For this article we used the REDSTICK shell-model code [5].

For Hartree-Fock plus RPA, we have used the SHERPA (shell-model RPA) code [6] that uses exactly the same input as REDSTICK. SHERPA places no restriction on the Hartree-Fock wave function except that it must be purely real; otherwise it can have any arbitrary deformation contained in the model space. Thus one can have spherical, axially symmetric deformation, triaxial deformation, and even parity-mixed ground state.

In previous articles we have used SHERPA to directly test HF+RPA as an approximation to full shell-model diagonalization, looking at correlation energies [7], ground-state observables [8], electromagnetic transitions [9], and charge-changing Gamow-Teller transitions [10]. In presenting those results we were frequently asked about the issue of the collapse of RPA. Such questions motivated this article.

III. FIRST- AND SECOND-ORDER TRANSITIONS

In this section we revisit Thouless's arguments [2,3] regarding the order of the transition. To do this, we need to remind the reader of at least one way to develop RPA [1], although we do not give the derivation in full.

Let $|\Psi\rangle$ be a Slater determinant, that is, an antisymmeterized product of single-particle wave functions. In second quantization, where $\hat{a}_a^\dagger$ creates a particle in state a, we write

$$|\Psi\rangle = \prod_i \hat{a}_i^\dagger |0\rangle. \tag{1}$$

We follow the usual convention where i, j denote occupied states and m, n denote unoccupied states. One then introduces the general particle-hole operator, $\hat{Z}^\dagger = \sum_{mi} z_{mi} \hat{a}_m^\dagger \hat{a}_i$, (where the z_{mi} can be complex) and the state

$$|z\rangle = \exp(\hat{Z})|\Psi\rangle, \tag{2}$$

which, by Thouless's theorem [3] is a Slater determinant not orthogonal to the starting state. One can compute

$$E(z) = \frac{\langle z|\hat{H}|z\rangle}{\langle z|z\rangle}, \tag{3}$$

which, assuming z small, can be expanded

$$E(z) = E_0 + \sum_{mi} h_{mi}^* z_{mi} + h_{mi} z_{mi}^* + \sum_{mi,nj} A_{mi,nj} z_{mi} z_{nj}^* + \frac{1}{2} B_{mi,nj} z_{mi}^* z_{nj}^* + \frac{1}{2} B_{mi,nj}^* z_{mi} z_{nj} + \cdots. \tag{4}$$

At a local minimum, $h_{mi} = 0$; this is the Hartree-Fock condition, and E_0 is the Hartree-Fock energy. The quadratic terms can be treated as a harmonic oscillator: one treats the z_{mi} as boson operators and using a Bogoliubov transformation put into diagonal form, using the famous RPA matrix equation:

$$\begin{pmatrix} \mathbf{A} & \mathbf{B} \\ -\mathbf{B}^* & -\mathbf{A}^* \end{pmatrix} \begin{pmatrix} \vec{X}_\lambda \\ \vec{Y}_\lambda \end{pmatrix} = \Omega_\lambda \begin{pmatrix} \vec{X}_\lambda \\ \vec{Y}_\lambda \end{pmatrix}. \tag{5}$$

There can be, of course, higher-order corrections in the energy landscape beyond quadratic, which we will consider shortly.

Suppose one is in a SC state, e.g., a state of good angular momentum, usually spherical, or parity. Then, solving Eq. (5) one finds the X, Y modes also have good symmetry. For example, with our code SHERPA, if the HF state is spherically symmetric, one gets out RPA modes that have good angular momentum J, and one sees the appropriate $(2J+1)$ degeneracy in the RPA frequencies Ω_λ. (If, however, rotational symmetry is broken but one has axial symmetry, then one can have two-fold degeneracies, signaling RPA modes that are time-reversed of each other, or a single mode, which must be time-reversal even. In the event of triaxiality, one has no degeneracies in the RPA spectrum.)

To consider "state transitions," from SC to SNC, one needs to look at higher-order terms. Let $\hat{Z}_\lambda$ represent generically the RPA modes; by expanding about the HF minimum, one expands the energy landscape by $\langle HF|\hat{Z}_\lambda^n|HF\rangle$. Because we are at a minimum, $n = 1$ vanishes. $n = 2$ yield the curvature and the RPA frequencies. What about $n = 3, 4, \ldots$?

Now we get to the heart of Thouless's argument. If the RPA mode $\hat{Z}_\lambda$ has odd parity, while the HF state has good parity, then $\langle HF|\hat{Z}_\lambda^n|HF\rangle$ must vanish for all odd n. However, if $\hat{Z}_\lambda$ has even parity, then $\langle HF|\hat{Z}_\lambda^3|HF\rangle$ can be nonzero; for example, it is possible to couple three $J = 2$ operators to total angular momentum zero.

Figure 1 illustrates both cases. Figure 1(a) is for modes with even parity so cubic terms play a role. One can clearly have coexisting local minima, and so one gets a first-order transition. Figure 1(b) is for odd-parity modes so the energy landscape must be symmetric. One tends to get only a second-order transition.

In our examples below, we see Thouless's predictions played out. A system with only even-parity modes has first-order transitions, while a system with odd-parity modes has a second-order transition.

What happens in a second-order transition? In that case the RPA frequencies $\Omega_\lambda \to 0$ and the fluctuations about the HF state, measured by $|Y_\lambda|$, become very large, allowed because the RPA vectors have a nonstandard normalization:

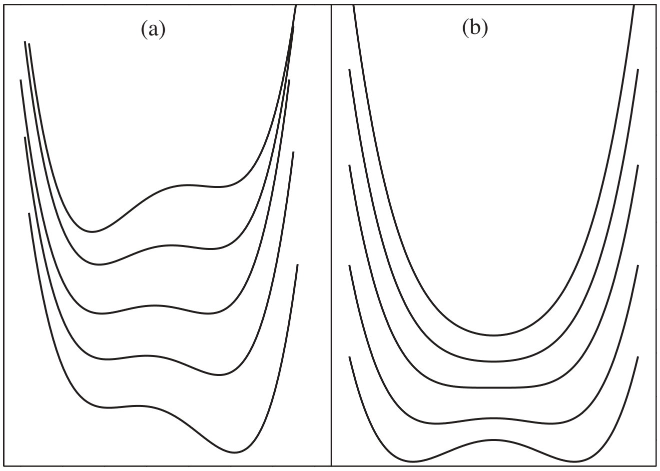

FIG. 1. Sketches of "phase" transitions in the energy landscape. (a) A first-order transition. (b) A second-order transition.

$|X_\lambda|^2 - |Y_\lambda|^2 = 1$. The RPA energy is

$$E_{\rm RPA} = E_{\rm HF} - \sum_{\lambda>0} \hbar\Omega_\lambda |Y_\lambda|^2 - \frac{\langle P^2\rangle}{2M_0} \quad (6)$$

(see Refs. [1,7] for details), and so as $|Y_\lambda|^2$ becomes large, the energy dives or collapses. The appearance of unphysical values is unsurprising because in the derivation one assumes small amplitudes for X and Y.

In the published literature, discussions regarding the behavior of the RPA near a phase transition focus exclusively on collapse of RPA [1,11], that is, on second-order transitions. Outside of Thouless [2] there is no discussion of first-order transitions (indeed, the literature appears to uniformly refer to phase transitions without quantifying the order of the transition). Yet, as illustrated below, it is not hard to find a first-order transition. It is possible that people using RPA have encountered first-order transitions without realizing it, as there is no catastrophic collapse to signal the transition. While clearly second-order transitions are more problematic, we find it instructive to explore both kinds.

IV. RESULTS

A. Example of a first-order transition: deformation

We begin with two case studies in the sd shell, using Wildenthal's universal sd (USD) interaction [12]. The first of these is ^{28}Si (six valence protons and six valence neutrons). By increasing the difference Δ between the $0d_{5/2}$ single-particle energy and the $1s_{1/2}$-$0d_{3/2}$ single-particle energies, we can force the Hartree-Fock state to go from an oblate deformed state to a spherical state with the $0d_{5/2}$ shell filled. For convenience $\Delta = 0$ corresponds to the original Wildenthal values.

Figure 2 shows the "exact" calculation, which is an interacting shell-model calculation performed in the full $0\hbar\omega$ sd valence space, compared to the lowest Hartree-Fock energy, and the RPA correlation correction on top of the HF energy. Because one switches between two degenerate HF states, the HF energy is continuous, while the HF+RPA energy is discontinuous, because the curvatures (RPA frequencies) are different. The right-hand panel illuminates in detail what is going on. Here we explicitly show the (oblate) deformed and spherical HF energies and their respective RPA corrections. One sees there is a significant region of parameter space, encompassing the original Wildenthal value, where locally stable deformed and spherical HF solution coexist.

As we drive Δ further positive or negative, eventually the deformed or spherical solutions, respectively, become unstable. In Fig. 2 this is seen as the HF+RPA energy dives sharply. For further diagnosis, in the upper half of Fig. 3 we plot the lowest nonzero RPA eigenfrequencies Ω as a function of Δ. (The deformed state also has two zero-frequency modes corresponding to broken rotational symmetries.) We see that one eigenfrequency dives to zero, signaling an instability. As further diagnosis, we give the degeneracy of the RPA eigenfrequencies; for the spherical HF state, the degeneracy of the collapsing eigenfrequency is 5, suggesting a quadrupole

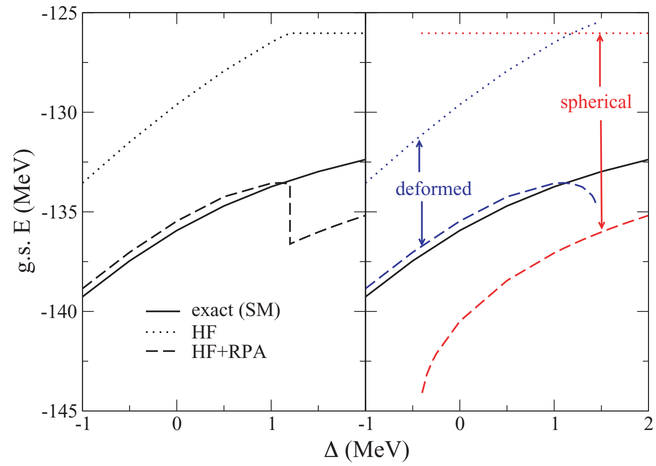

FIG. 2. (Color online) Ground-state energy of ^{28}Si, calculated in the full interacting shell model (SM, solid lines), Hartree-Fock (HF, dotted lines), and Hartree-Fock plus random-phase approximation (HF+RPA, dashed lines). Here Δ is added to the $1s_{1/2}$ and $0d_{3/2}$ single-particle energies; $\Delta = 0$ corresponds to the original Wildenthal values. The left-hand panel shows only the final result; the right-hand panel identifies spherical and (oblate) deformed mean-field phases. Note the significant region of coexistence.

mode. For the oblate deformed state, the RPA eigenmodes either come in time-reversed pairs (degeneracy = 2) or are already time-reversal-even (degeneracy = 1).

Note: We cannot follow the RPA frequency all the way to zero, due to numerical instabilities, although the trend is clear. Though we do not plot it, we also get a corresponding eigenvalue of the the stability matrix diving to zero.

As the RPA frequency dives to zero, the corresponding magnitude of the hole-particle amplitude, $|Y_\lambda|^2 = \sum_{mi} |Y_{mi,\lambda}|^2$, increases dramatically. This we plot in the lower half of Fig. 3. As discussed in a previous section, it is this increase in $|Y|$ that causes the correlation energy to take on unphysically

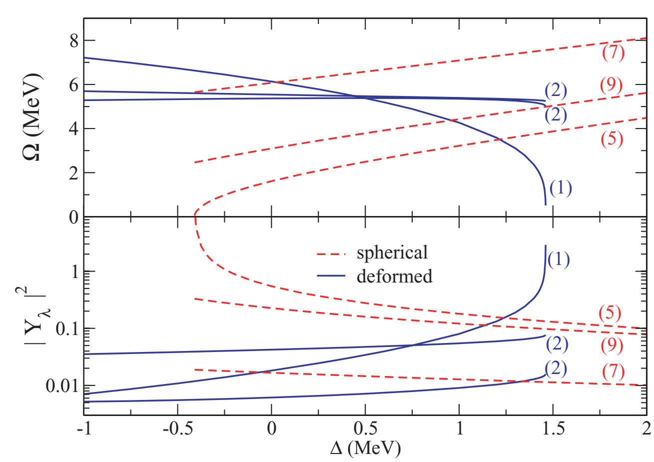

FIG. 3. (Color online) For ^{28}Si. (Upper panel) Low-lying RPA frequencies Ω for spherical (dashed) and deformed (solid) HF states. (Lower panel) $|Y_\lambda|^2$ corresponding to the RPA frequencies in the upper panel. In both cases the degeneracy is given in parentheses; for the spherical case the degeneracy $= 2J + 1$ where J is the angular momentum of the RPA mode.

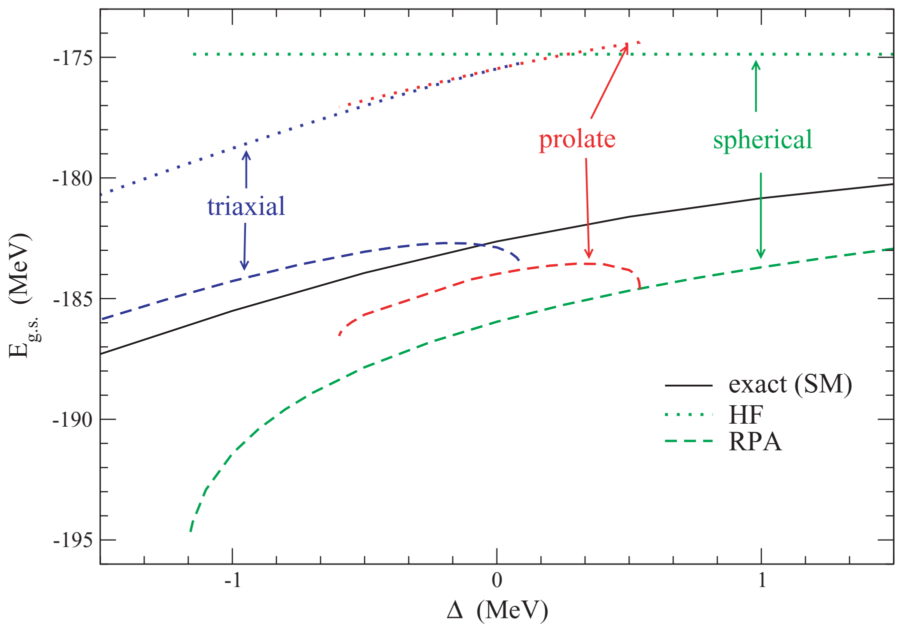

FIG. 4. (Color online) Similar to Fig. 2 but for ^{32}S; here Δ is the change in the $0d_{3/2}$ energy.

large values. Although we do not show it, we have also computed the expectation value for various operators, such as the $Q \cdot Q$ operator; while the HF contribution is stable, the RPA correlation correction [8] also shows unphysically large values.

We also considered ^{32}S, that is, eight valence protons and eight valence neutrons, and drove the $0d_{3/2}$ single-particle energy up and down. This case was very interesting because we could get, by adjusting Δ, spherical, prolate, and triaxial solutions. Figure 4 shows the shell-model (SM), Hartree-Fock, and HF+RPA energies for the ground state, while Fig. 5 shows the RPA frequencies and $|Y_\lambda|^2$. While a $J = 2$ (degeneracy $= 5$) eigenfrequency is falling, a $J = 4$ (degeneracy $= 9$) mode actually falls below it, suggesting that ultimately it is a hexadecupole mode becomes unstable first. The prolate state has both degenerate (time-reversed pairs) and nondegenerate states; the triaxial state, which has broken all possible symmetries, has no degenerate RPA modes.

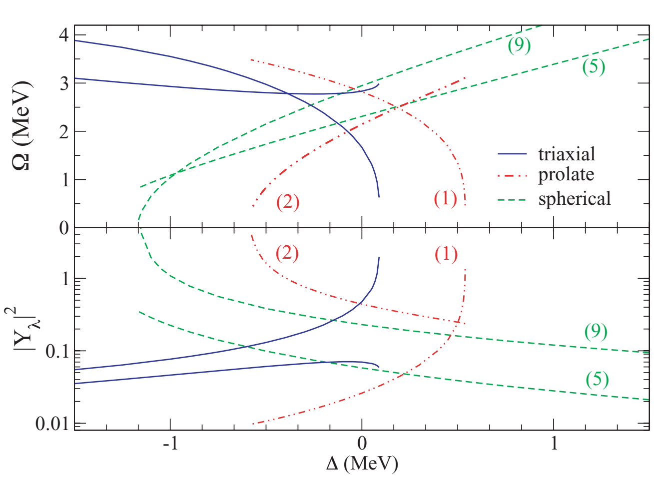

FIG. 5. (Color online) Similar to Fig. 3 but for ^{32}S; here Δ is the change in the $0d_{3/2}$ energy.

We reiterate: The key idea here is that the coexistence of locally stable phases leads to a first-order transition. The stable phases coexist easily because the parity-conserving mode—here quadrupole—means one can have cubic as well as quartic terms in the energy landscape. When we have an odd-parity mode, as illustrated in the next session, cubic terms are suppressed and one gets a second-order transition.

B. Example of a second-order transition: parity-mixing

Second-order transitions lead to collapse of RPA. The classic example is the Lipkin model, which in its original form has a conserved parity (the Lipkin model is a two-level system, and the original Lipkin interaction could only promote or demote two particles at a time, thus providing an parity-like symmetry: either an even or an odd number of particles in the upper level); the transition of the HF state in the Lipkin model was from an exact parity state, with all particles in the lower level, to a mixed parity state.

For our examples of second-order transitions, we consider a case involving shells of opposite parity. We fix the $0s$ shell to be a closed core and have as the valence space $0p_{3/2}$, $0p_{1/2}$, and $0d_{5/2}$, $1s_{1/2}$. We look at ^{12}C, with four valence protons and four valence neutrons, without any truncations on the many-body space. (The only reason we leave out the $0d_{3/2}$ orbit is to make full shell-model calculations tractable; SHERPA can easily handle the full p-sd space, but the HF+RPA results look very similar to what we present here. We also have looked at ^{16}O and ^{20}Ne in similar spaces and get similar results.) We use the Cohen-Kurath (CK) matrix elements in the $0p$ shell [13], the USD interaction [12] in the $0d_{5/2}$-$1s_{1/2}$ space, and the

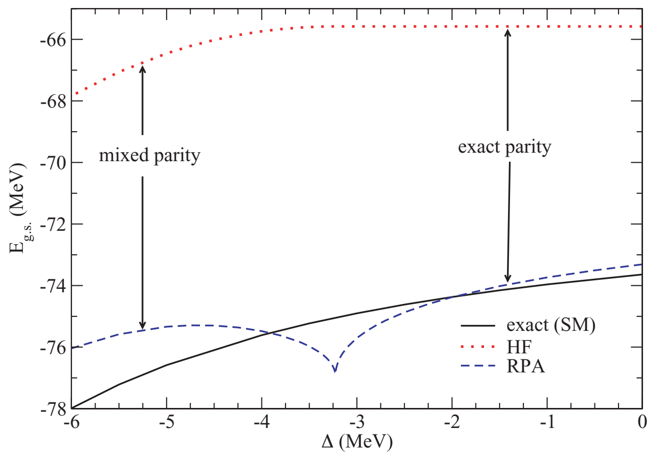

FIG. 6. (Color online) Ground-state energy of ^{12}C in the $0p_{1/2}$-$0p_{1/2}$-$0d_{5/2}$-$1s_{1/2}$ space, calculated in the full interacting shell model (SM) (solid line), Hartree-Fock (HF) (dotted line), and Hartree-Fock plus random-phase approximation (RPA) (dashed line). Here Δ is added to the $1s_{1/2}$ and $0d_{5/2}$ single-particle energies; $\Delta = 0$ puts the negative-parity states in the SM at approximately the correct location. We show where the HF states and corresponding HF+RPA states have either exact parity (and also spherical symmetry) or mixed parity (and break rotational invariance as well).

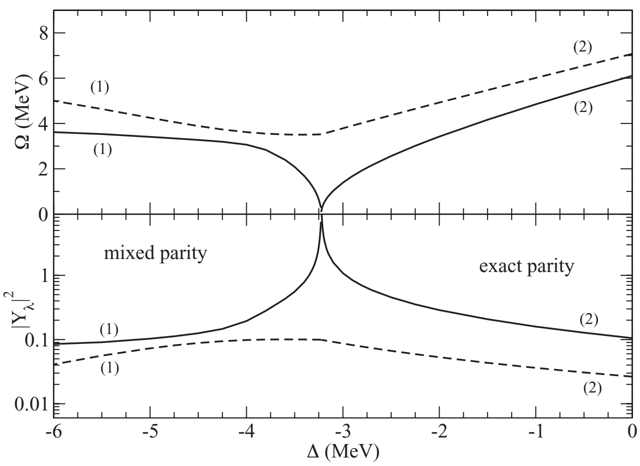

FIG. 7. For ^{12}C. (Upper panel) low-lying RPA frequencies Ω for exact-parity and parity-mixing HF states. (Lower panel) $|Y_\lambda|^2$ corresponding to the RPA frequencies in the upper panel. In both cases the degeneracy is given in parentheses; the exact-parity HF states are oblate, allowing for time-reversed pairs, but for parity-mixing the HF state becomes triaxial, breaking the time-reversal degeneracy.

Millener-Kurath (MK) p-sd cross-shell matrix elements [14]. Within the p and sd spaces we use the original spacing of the single-particle energies for the CK and USD interactions, respectively, but then shift the sd single-particle energies up or down relative to the p-shell single particle energies by an amount Δ; we define $\Delta = 0$ where we get the first 3^- state at approximately 6.1 MeV above the ground state. The rest of the spectrum, in particular the first excited 0^+ state, is not very good, but the idea is to have a nontrivial model, not an exact reproduction of the spectrum. (As a side note, this model space is not translationally invariant, and so we do *not* get zero-frequency modes from broken translational invariance.)

Figure 6 compares the exact SM ground-state energy with HF and HF+RPA. Here the HF+RPA energy dives, or "collapses" at the transition point. A more detailed look is in Fig. 7, which plots the RPA frequencies.

In Fig. 7 we also show the RPA eigenfrequencies and the magnitude of $|Y_\lambda|$. The exact-parity HF states are oblate so the RPA frequencies come in degenerate pairs from time-reversal symmetry. The mixed-parity HF states are triaxial, breaking time-reversal degeneracy.

V. CONCLUSIONS

We have applied Hartree-Fock plus the random-phase approximation in the framework of the interacting shell model, with complicated, realistic forces. By changing the single-particle energies we could drive the Hartree-Fock solution between symmetry conserving and symmetry nonconserving states. In accordance with Thouless's original, and oft-forgotten, analysis, first-order transitions are associated with even-parity modes, such as the quadrupole mode, and do not display, at the transition point, the infamous collapse of RPA. Instead, one obtains the collapse of RPA only in second-order transitions, associated with odd-parity modes. The latter are of course more serious, but it is useful to keep in mind that not all state or phase transitions automatically lead to the collapse of RPA.

ACKNOWLEDGMENTS

The US Department of Energy supported this investigation through Grants DE-FG02-96ER40985 and DE-FC02-07ER41457.

[1] P. Ring and P. Shuck, *The Nuclear Many-Body Problem*, 1st ed. (Springer-Verlag, New York, 1980).
[2] D. J. Thouless, Nucl. Phys. **22**, 78 (1961).
[3] D. J. Thouless, Nucl. Phys. **21**, 225 (1960).
[4] H. Lipkin, N. Meshkov, and A. J. Glick, Nucl. Phys. **62**, 188 (1965).
[5] W. E. Ormand (private communication).
[6] I. Stetcu, Ph.D. thesis, Louisiana State University, 2003.
[7] I. Stetcu and C. W. Johnson, Phys. Rev. C **66**, 034301 (2002).
[8] C. W. Johnson and I. Stetcu, Phys. Rev. C **66**, 064304 (2002).
[9] I. Stetcu and C. W. Johnson, Phys. Rev. C **67**, 044315 (2003).
[10] I. Stetcu and C. W. Johnson, Phys. Rev. C **69**, 024311 (2004).
[11] C. Federschmidt and P. Ring, Nucl. Phys. **A435**, 110 (1985); J. G. Hirsch, P. O. Hess, and O. Civitarese, Phys. Lett. **B390**, 36 (1997); J. Engel, S. Pittel, M. Stoitsov, P. Vogel, and J. Dukelsky, Phys. Rev. C **55**, 1781 (1997); J. G. Hirsch, P. O. Hess, and

O. Civitarese, *ibid.* **56**, 199 (1997); A. Mariano and J. G. Hirsch, *ibid.* **57**, 3015 (1998); **58**, 2736 (1998); J. G. Hirsch, O. Civitarese, and M. Reboiro, *ibid.* **60**, 024309 (1999); F. Šimkovic, A. A. Raduta, M. Veselsky, and A. Faessler, *ibid.* **61**, 044319 (2000); A. Mariano and J. G. Hirsch, *ibid.* **61**, 054301 (2000); N. Dinh Dang and V. Zelevinsky, *ibid.* **64**, 064319 (2001); N. D. Dang, *ibid.* **71**, 024302 (2005).

[12] B. H. Wildenthal, Prog. Part. Nucl. Phys. **11**, 5 (1984).

[13] S. Cohen and D. Kurath, Nucl. Phys. **73**, 1 (1965).

[14] D. J. Millener and D. Kurath, Nucl. Phys. **A255**, 315 (1975).